CrossMark

Effect of Cu Interlayer on the Microstructure and Strength for Brazing of Tungsten/316L Steel

Meng Wang, Yuanting Chen, Xianfen Li, Peng Hua, Linfeng Gao, Wei Zhou, and Yucheng Wu

Brazing is an effective technique for joining tungsten and steel. However, the high residual stresses are produced due to the different coefficients of thermal expansions between tungsten and steel. Compared with the direct brazing with BNi-2 foil filler, BNi-2/Cu/ BNi-2 multiple interlayer was used as filler to minimize the residual stresses between tungsten and 316L steel. The brazing experiments were conducted at 1050 °C for 25 min using Cu foils with different thickness. The results show that tungsten and 316L steel have been successfully joined by brazing. The intermetallic compound of NiW formed at the W/BNi-2 interface, which was detrimental to the strength of the joint. The microhardness of different diffusion zones is higher than that of the substrates owing to the formation of intermetallic compound and solid solution. All specimens of shear testing fractured at the W/BNi-2 interface close to W substrate, and the average strength of joints was 197, 275 and 268 MPa with multiple interlayer thickness of 0.2 , 0.1 and 0.05 mm copper foil, respectively, while the average strength of joints was 143 MPa with BNi-2 foil filler. The significant increase in the joint shear strength can be ascribed to the Cu foil in the multiple interlayer because of with excellent plasticity and toughness.

Keywords	316L steel, brazing, microstructure, shear strength, tungsten

1. Introduction

Divertor works in a complicated environment with high heat flux, high particle flux and heavy neutron irradiation (Ref 1). Appropriate plasma facing material (PFM) is important to enhance the lifetime of the component itself (Ref 2). Due to the advantages of low activation, high Z material, high thermal conductivity, high sputtering resistance and low deuterium/ tritium retention (Ref 3, 4), tungsten is considered as one of the most promising divertor materials. However, tungsten is difficult to machine due to its brittle nature at room temperature. For a divertor, tungsten and steel usually used as first wall material and structural material, respectively. The joining of these two materials is essential to a divertor (Ref 5). Due to their huge differences in physical properties of these two materials, such as different melting points (Tm: 3407 °C for tungsten and 1300-1500 °C for steels) and large mismatch of coefficients of thermal expansion (CTE: 4.5×10^{-6} k^{-1} for tungsten and $10\text{-}18 \times 10^{-6}$ k^{-1} for steels), large residual stresses appear along the bonding interfaces. Therefore, traditional fusion welding is inapplicable to join tungsten and steels. It has been reported that brazing and solid-state diffusion bonding have been an ideal method to join tungsten and steels.

In solid-state diffusion bonding process (Ref 6-8), the interlayer is widely used to reduce the residual stresses. Compared with the direct diffusion bonding (Ref 9), the property of the joints is significantly improved by inserting interlayer. For instance, Zhong et al. (Ref 6, 10) used Ti and Ni as the interlayer to bond tungsten and steels. The brazing joint (Ref 11-13) was successfully obtained by using the nickel-based filler with excellent wettability and mobility, however, the investigation of the interlayer was insufficient. In this work, a copper interlayer with characteristics of low yield strength and low elastic modulus (Ref 14) was inserted between nickel-based fillers to reduce the residual stress in the joints. The interface microstructure, microhardness and mechanical properties of brazing joints with BNi-2/Cu/BNi-2 multiple interlayer were analyzed.

2. Experimental Procedures

The pure tungsten (99.95 wt.%) and 316L steel (Fe-17Cr-13Ni-3Mo-2Mn, wt.%) used in this work were cut by wire-electrode cutting to a dimension of 10 mm^L × 10 mm^W × 5 mm^T. Meanwhile, commercial copper interlayer (99.9 wt.% purity) with different thickness (0.05, 0.1, 0.2 mm) and a 0.03 mm thick BNi-2 filler (Ni-6Cr-5Si-3.5Fe-3.5B, wt.%. solidus temperature 971 °C, liquidus temperature 999 °C) were cut to a size of 10 mm × 10 mm. Before the brazing process, the surfaces of these specimens were ground with SiC emery paper and polished with diamond suspension. To remove the oil contamination, the samples were cleaned in an ultrasonic acetone bath for 15 min. As shown in Fig. 1, the 316L/W joint was brazed in a molybdenum wire vacuum furnace by using BNi-2 interlayer and BNi-2/Cu/ BNi-2 multiple interlayer, respectively. Since the brazing temperature was generally 50 °C higher than the filler's liquidus temperature, the brazing was carried out at 1050 °C. The thermal cycle of the brazing

Meng Wang, Yuanting Chen, Xianfen Li, Peng Hua, Linfeng Gao, and **Yucheng Wu,** School of Materials Science and Engineering, Hefei University of Technology, No.193, Tunxi Road, Hefei 230009, China; and **Wei Zhou,** School of Mechanical and Aerospace, Nanyang Technology University, 50 Nanyang Avenue, Singapore 639798, Singapore. Contact e-mail: lxfytt@163.com.

process was as follows: firstly heated to 800 °C with heating rate of 10 °C/min, then increased to the target brazing temperature with heating rate of 10 °C/1.5 min, held at the brazing temperature for 25 min under vacuum ($< 10^{-3}$Pa), and finally cooled to room temperature within the furnace.

The cross sections of brazing bonded joints were cut and prepared for metallographic examination. The microstructure observation was carried out under field-emission scanning electron microscope (SEM). The chemical composition and phase analysis of the joints was analyzed with energy-dispersive x-ray spectrometry (EDS) and XRD. The mechanical property of bonded joints was evaluated by shear test (specimens size: 4 mm^L × 3 mm^W × 3 mm^T, presented in Fig. 2) on CMT5150 Universal tester with a constant displacement rate of 0.5 mm/min. The average strength of five specimens test results was recorded and the fractured surfaces were examined. Microhardness was tested across the bonding interface by VTD401 microhardness tester with a holding time of 15 s and a load of 100 g.

3. Results and Discussion

3.1 Microstructural Investigation of the Joints

The brazing between W and 316L was successfully carried out. No cracks and unbounded regions were observed along the joint bonding interfaces. The micrographs and EDS line scan results of the different joints are presented in Fig. 3 and 4, respectively. It reveals that each joint is composed of several layers.

3.1.1 The Analysis of the 316L/W Joint with BNi-2/Cu/ BNi-2 Multiple Interlayer. Figure 3(a) shows back-scattered electron image of 316L/Cu/W with BNi-2/Cu/ BNi-2 multiple interlayer. The microstructure of 316L/BNi-2/Cu interface and Cu/ BNi-2/W interface are shown in Fig. 3(b) and (c), respectively.
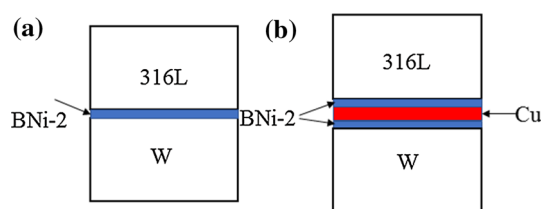
Fig. 1 A schematic description of joint models: (a) 316L/W, (b) 316L/Cu/W
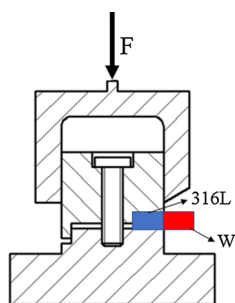
Fig. 2 A schematic description of shear test configuration

As for the 316L/BNi-2/Cu interface, 316L/filler diffusion layer (D1), filler (D2), filler/Cu diffusion layers (D3) are produced. As for the Cu/BNi-2/W interface, it includes Cu/filler diffusion layer (D4), filler (D5), filler/W diffusion layer (D6). Apparently, these diffusion layers are produced during the brazing process due to the interdiffusion effect. As a result of the elements diffusion from the filler to the 316L steel during brazing, the intergranular infiltration occurs in the 316L near the D1 region.

The elemental composition at Point A consist of 62.17 at.% Ni, 5.68 at.% Cr, 3.56 at.% Fe, 1.54 at.% W, 11.07 at.% Si, 15.98 at.% Cu, which is similar to Point C. This confirmed the formation of Nickel-based solid solution in this region. The elemental composition at Point B consist of 31.18 at.% Cr, 66.17 at.% B, 0.26 at.% Si, 0.53 at.% Cu, 0.38 at.% Fe, 1.48 at.% Ni. It should be noted that the boron (B) content may be not exactly detected by EDS because boron is light element. It is also observed that the Cr profile shows steep fluctuation in D2 zones (as shown in Fig. 4a), which may be attributed to the formation of Cr-B intermetallic compounds (CrB, Cr_5B_3, Cr_2B) (Ref 15). At Point D, we detected approximately 11.4 at.% Cr, 33.9 at.% Ni and 54.7 at.% W. According to the W-Ni binary diagram, (shown in Fig. 5) the composition at Point D is located at the area between NiW and NiW_2 intermetallic compound. The presence of NiW and Ni(W) phase is confirmed by XRD, as shown in Fig. 6. Additionally, a small amount of Cr elements has been dissolved in NiW intermetallic compound.

Although the same fillers are used in this work, it is interesting to find that the thickness of the filler (D2) becomes thicker than that of filler (D5). The different thickness of fillers can be explained as follows: (1) copper can improve the wettability of BNi-2 filler (Ref 16). Fe and Ni/Cu/Ni exhibit good compatibility, while Ni and W are not compatible well. (2) The melting point of tungsten (3040 °C) is much higher than the brazing temperature (1050 °C), hence the tungsten atom is relatively difficult to be activated.

3.1.2 The Analysis of the 316L/W Joint with BNi-2 Filler. Figure 7(a) shows back-scattered electron image of 316L/BNi-2/W. The high magnification image of 316L/BNi-2/ W interface and the EDS line scan results are shown in Fig. 7(b) and (c), respectively.

As for the 316L/W bonded joint, there are three diffusion layers formed during brazing process: 316L/filler diffusion layer (A1), filler (A2), filler/W diffusion layer (A3). The chemical composition at Point E consist of 70.22 at.% Ni, 5.93 at.% Cr, 4.94 at.% Fe, 8.47 at.% W, 10.43 at.% Si, confirming the formation of Nickel-based solid solution. At Point F, chemical composition of 10.2 at.% Cr, 36.6 at.% Ni and 53.2 at.% W also indicated the formation of intermetallic compound between NiW and NiW2. This is confirmed by XRD analysis, as shown in Fig. 8.

Two types of compound appearing 'white' are observed: a continuous layer approaching W substrate and several discontinuous areas distributed in the filler (A2). This can be related to the growth process of intermetallic compound. Because plenty of vacancies and dislocations on the W substrate surface can provide the nucleation sites, the intermetallic compound grows along the W surface. When the intermetallic compound continues to grow, the direction of growth becomes horizontal.
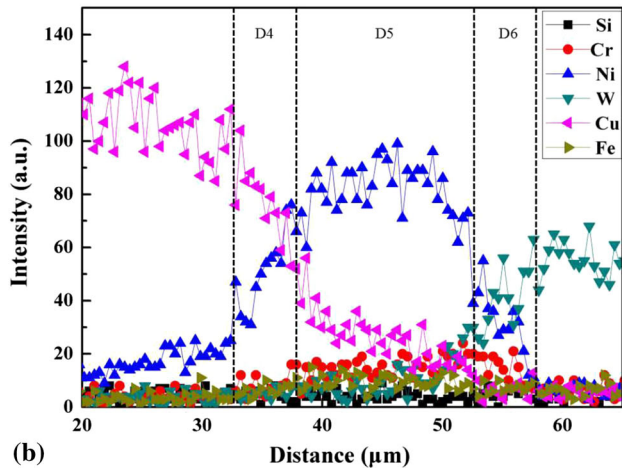
According to the NiW binary phase diagram (Ref 17), three types of intermetallic compound (Ni_4W, NiW, NiW_2) are stable.
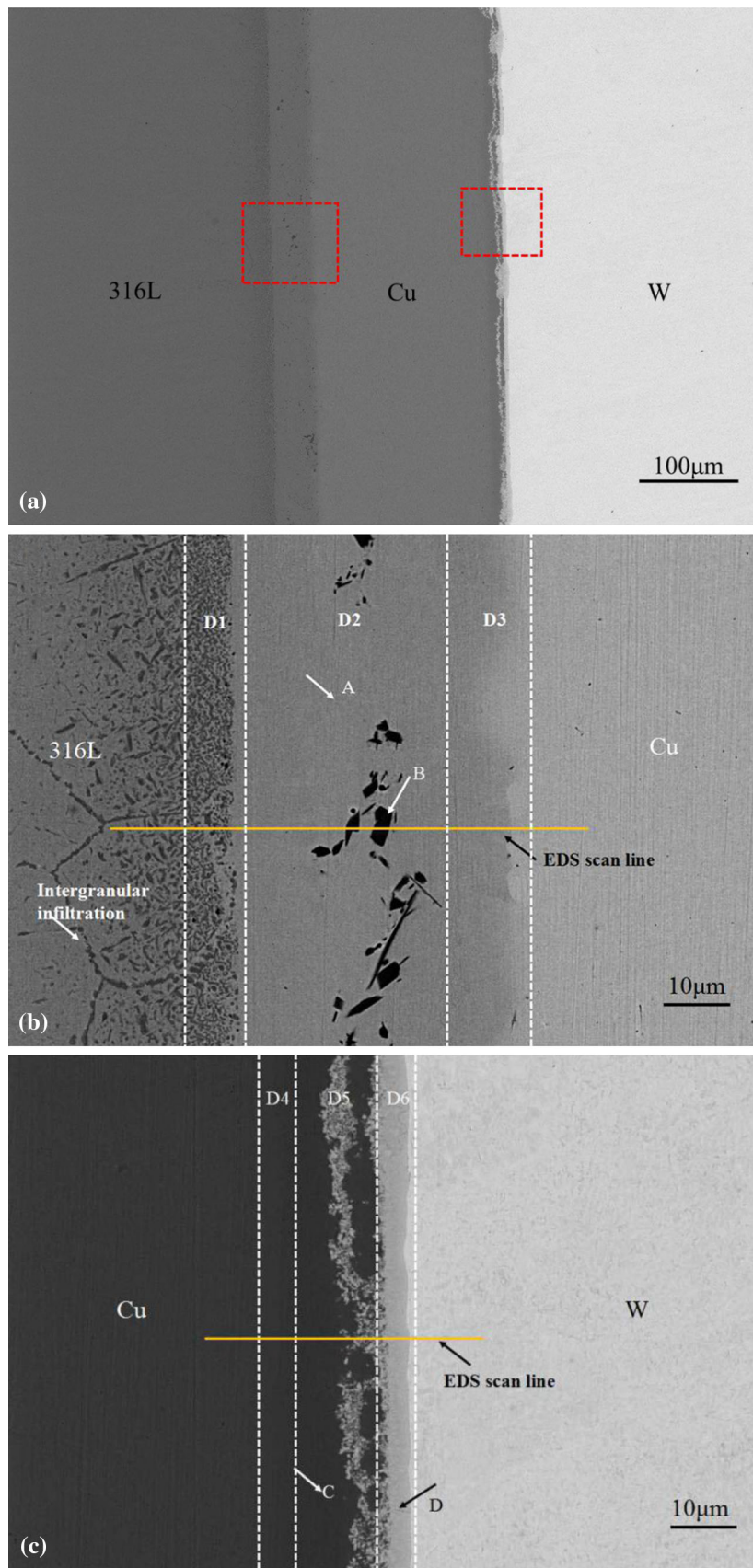
Fig. 3 Back-scattered electron micrographs of the joint with copper interlayer (0.2 mm thickness). (a) General view; (b) High magnification of the 316/Cu interface; (c) High magnification of the Cu/W interface
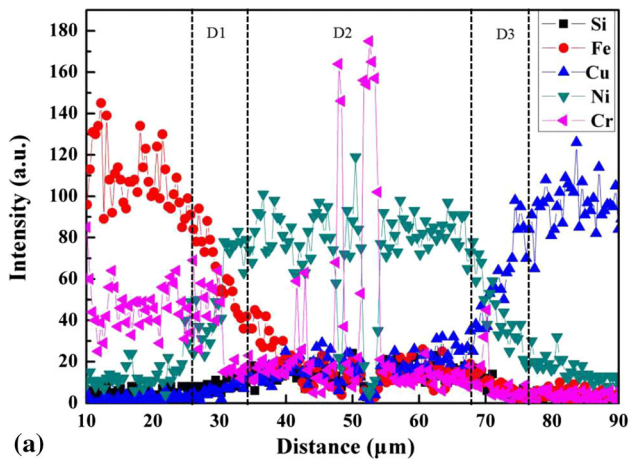
Fig. 4 EDS line scan results of the joint with copper interlayer (0.2 mm thickness) (a) EDS line scan results of 316L/BNi-2/Cu interface; (b) EDS line scan results of Cu/BNi-2/W interface

However, NiW_2 and Ni_4W are not identified in the present work. For the growth of intermetallic compounds, many investigations are carried out (Ref 18-21). Some researchers (Ref 1, 18-21) state that the growth rate of compound is related to the interdiffusion coefficient. In other words, if the interdiffusion coefficient for one intermetallic compound is much smaller than for other compounds, the intermetallic compound cannot grow up. The NiW is also observed by Walsh and Donachie (Ref 22) at 1273 K for 100 h and at 1311 K for 112-600 h. These imply that the interdiffusion coefficient is much smaller for Ni_4W and NiW_2 than for NiW. According to Ref. (Ref 20), however, Ni_4W, NiW and NiW_2 are formed by annealing at $T = 1073$-1273 K, $T = 1073$-1363 K and $T = 1073$-1313 K, respectively. In summary, the opinions between researchers are inconsistent due to different experimental parameters. Meanwhile, the mentioned-above joining
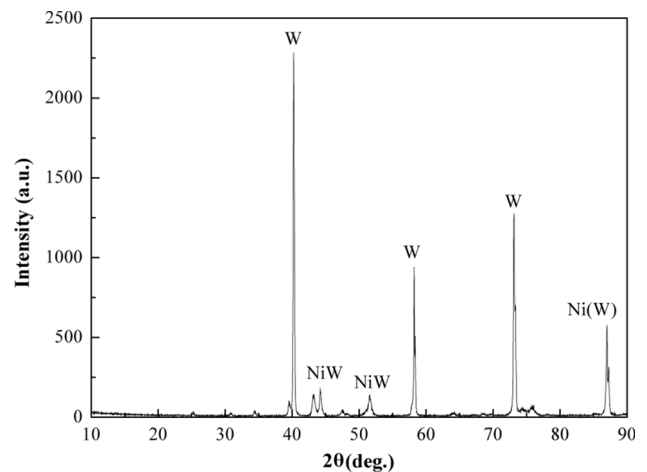
Fig. 6 XRD pattern of the fracture surface on W side for 316L/Cu/W (0.2 mm thickness copper interlayer)
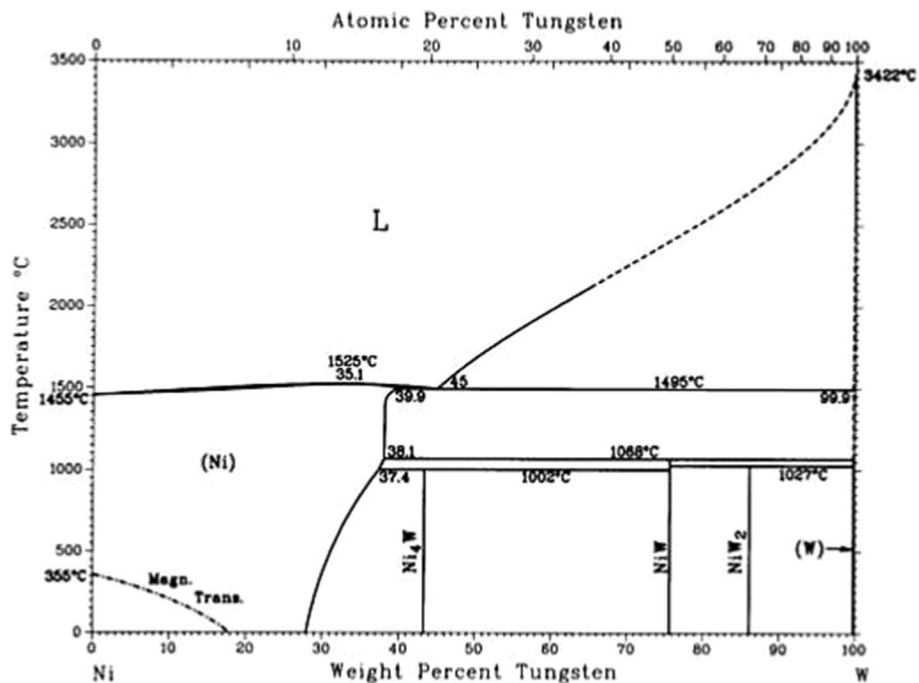
Fig. 5 NiW binary phase diagram
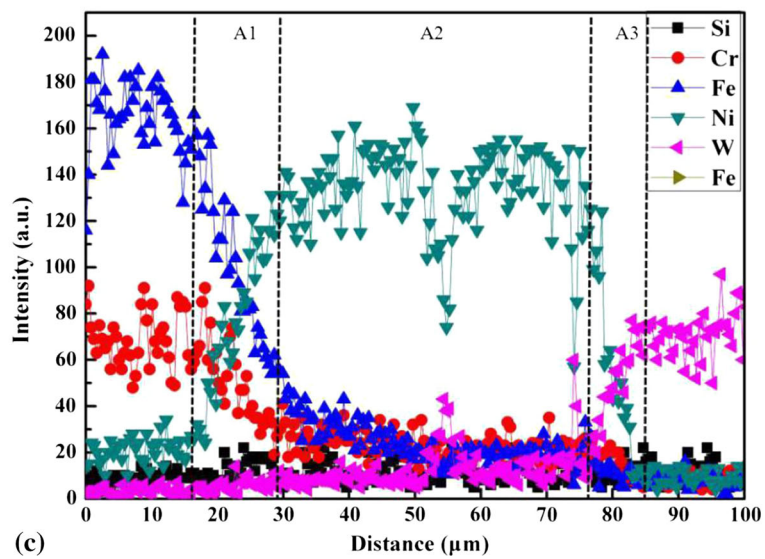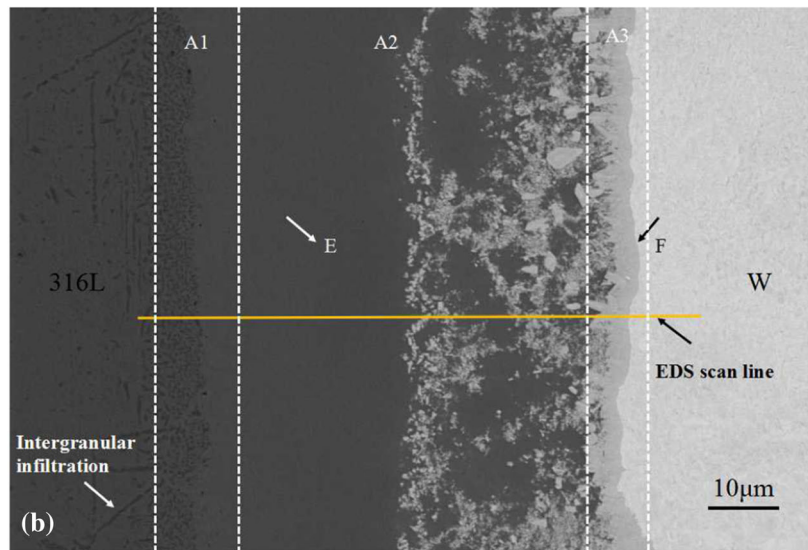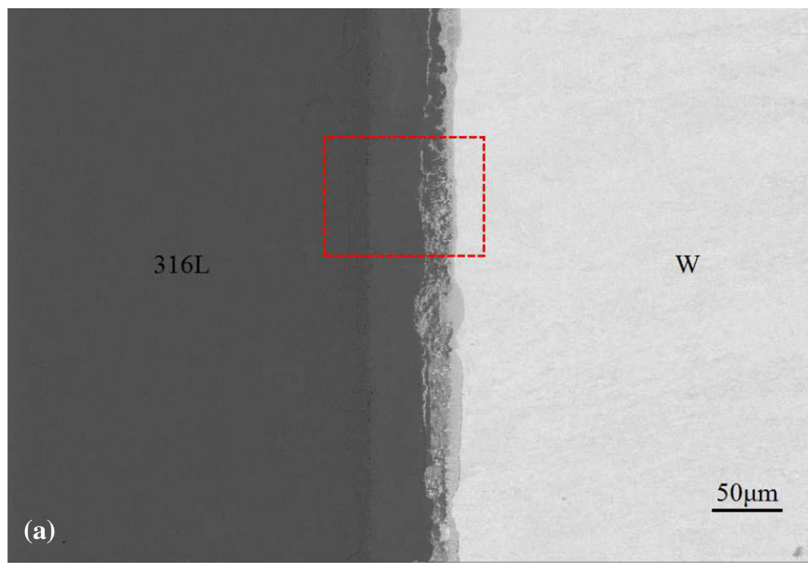
Fig. 7 Back-scatter electron micrographs and elemental intensity profiles of the joint without copper interlayer (a) general view; (b) High magnification detail of the 316L/W interface; (c) elemental intensity profiles of 316L/W

experiments are all conducted by solid diffusion bonding. For brazing, the growth of intermetallic compound is not investigated in depth (Ref 11-13). In the present work, the NiW may form due to the change of the interdiffusion coefficient. Compared with pure Ni foil used as a interlayer in solid diffusion bonding, BNi-2 filler in our work contains nickel element, boron, silicon. These elements may influence the interdiffusion coefficient. To understand the growth of intermetallic compounds, more work about interdiffusion coefficient should be done in the future.

3.2 Microhardness Across the Interfaces

Microhardness is tested on the polished cross section of the brazed joint for the 316L/Cu/W and 316L/W, respectively. The substantial variation indicates the changes in microhardness across profiles of the 316L/Cu/W and 316L/W, as displayed in Fig. 9 and 10, respectively.

In D1 and A1 regions, the microhardness increases due to formation of Ni-Fe solid solution. In spite of the formation of Cu-Ni solid solution in D3 and D4 regions, the hardness of Cu-Ni solid solution is lower than of the Fe-Ni solid solution. The

highest microhardness within the joint (600 HV) is located in the area next to W for 316L/Cu/W joint, indicating the formation of intermetallic compound. This is also verified by EDS and XRD results. The hardness value of the 316L near the joint interface is higher than that of the initial 316L ($<$ 200 HV) due to the penetration of BNi-2 filler into the grain boundary.

3.3 Shear Strength and Fracture Surface Analysis

The specimens for shear testing cut from the bonded joints are tested in CMT5150 Universal tester and five testing results are obtained for each specimen. The results shown in Fig. 11 indicate that the strengths of joint with copper interlayer are higher than that of the joint without a copper interlayer. It is advised that that soft copper interlayer can absorb some residual stresses along the joints during brazing (Ref 22). Zhang et al. (Ref 23) simulated the effect of interlayer with different thickness on the residual stress between Al_2O_3 and SS304 stainless steel, which showed that the residual stress of the joint decreased rapidly with the increase in the thickness of the interlayer at first and then the residual stress slowly
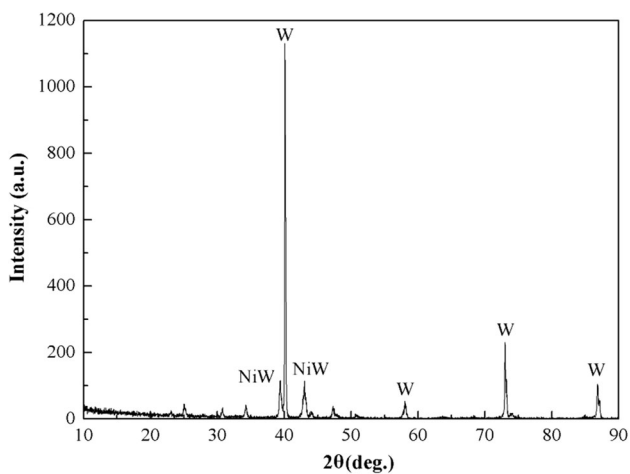

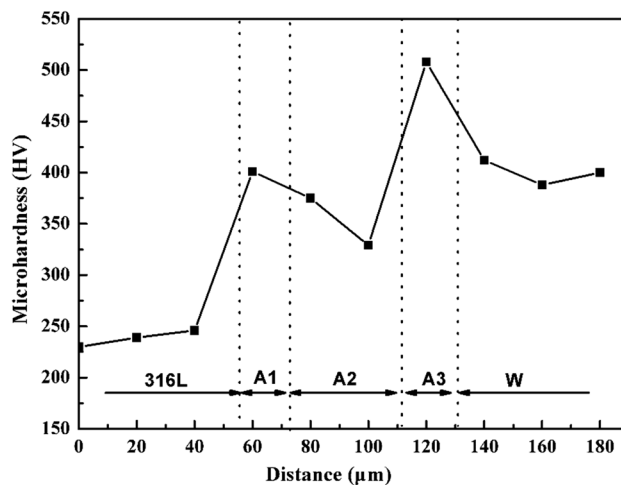**Fig. 8** XRD pattern of the fracture surface on W side for 316L/W joint

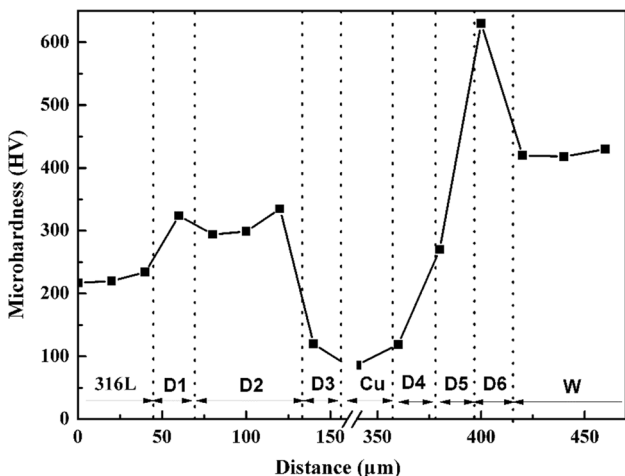**Fig. 10** Microhardness distribution 316L/W joint

Fig. 9 Microhardness distribution 316L/Cu/W joint (0.2 mm thickness copper interlayer)
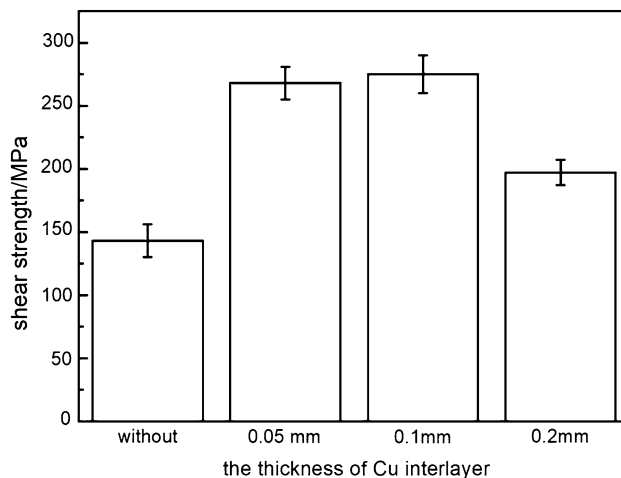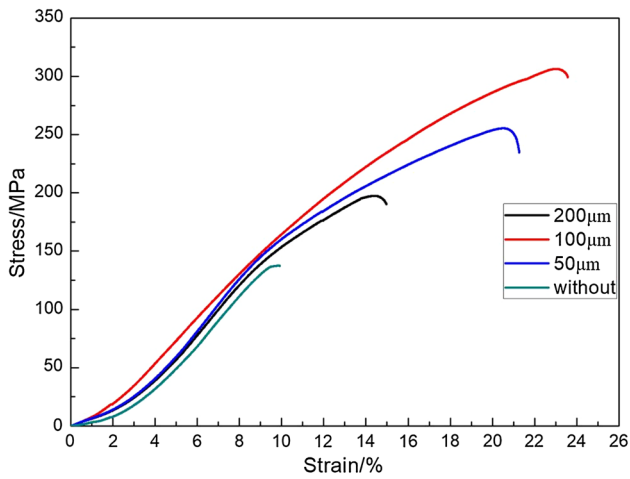

Fig. 11 Shear strength of the joints with different thickness of copper interlayer

Fig. 12 Stress–strain curves of shear testing on 316L/Cu/W joints with different thickness of copper interlayer

Fig. 13 Fracture surfaces of the 316L/Cu/W joint (0.2 mm thickness copper interlayer)

Fig. 14 Fracture surfaces of the 316L/W joint

decreased when the thickness of the interlayer reached a certain extent. Park (Ref 24, 25) simulated the strain energy distribution in ceramic-to-metal joints with multi-interlayer and different interlayer order, which confirmed that the increase in joint strength was due to the reduction of strain energy. In our work, it can be deduced that approximate 0.1 mm thickness copper interlayer might decrease the joint residual stress and the strain energy efficiently. Additionally, the diffusion of Cu into Ni-based filler can improve the wettability and mobility of BNi-2 filler (Ref 16). Considering these changes of brazing filler, the amount of solid solution and the width of diffusion zone, and the change of residual stress and strain energy, the shear strength of joints with Cu interlayer are increased in our work. From the point of welding structure mechanics, when the copper interlayer thickness is appropriate, the amount of Cu-based solid solution and the rest of softer Cu are proper to improve the joint strength. When the copper interlayer is too thick, the amount of the rest softer Cu increases in the joint, which will decrease the joint strength; if the copper interlayer is too thin, most of the area in the joint is fulfilled with Cu-based solid solution, which will limit the plastic deformation ability of joint. In our experiments, the shear strength of the joint with 0.2 mm copper interlayer is lower than that of 0.1 mm and 0.05 mm thickness, which show that the appropriate thickness of Cu interlayer is approximately 0.1 mm. Zhu (Ref 26) and Erskine (Ref 27) also indicated that the shear strength increased firstly and then decreased with the increase in the interlayer thickness. As shown in Fig. 12 in our work, the toughness of the joint is greatly improved by the addition of copper interlayer and 0.1 mm thickness copper interlayer is the optimal.

The microstructures of the typical fracture surface of the 316L/Cu/W joint and 316L/W joint are shown in Fig. 13 and 14, respectively. The fracture surface of the 316L/W joint is characterized by the appearance of the faceted grains (region G) and river patterns (region H). The average composition of region G is 99.92 at.% W, 0.08 at.% Ni, which suggests Region G is located on the substrate W adjacent to the brazing seam. While Region H is composed of 59.56 at.% W, 40.44 at.% Ni, the NiW can be expected in this region by XRD. For the fracture surface of 316L/Cu/W joint, in addition to faceted grains (region I) and river patterns (region J), dimples (region
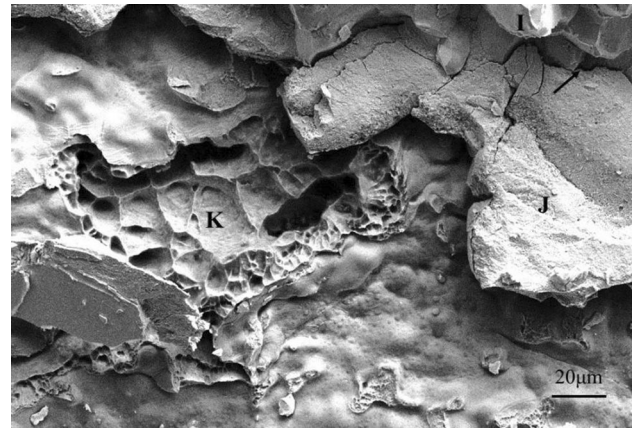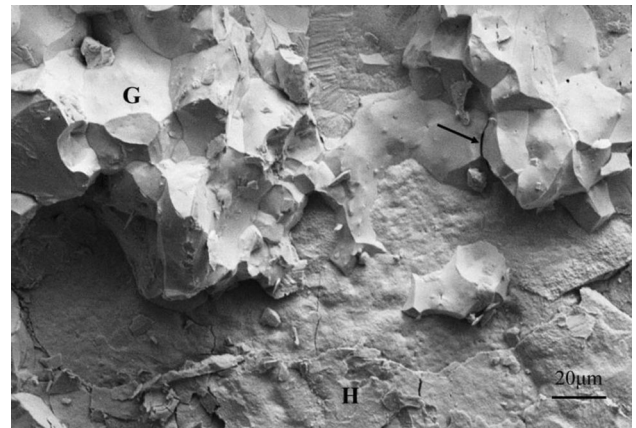
K) are visible on the fracture surface. The average element content of Region I and Region J is similar to the element content in Region G and Region H, respectively, suggesting that Region I is in W near the brazing seam and Region J is NiW. Region K is composed of 80.22 at.% Ni, 5.93 at.% Cr, 13.85 at.% W, and Nickel-based solid solution can be expected in this region. On the base of the above discussion, it can be concluded that the fracture mode of 316L/W is brittle fracture, while the fracture mode of 316L/Cu/W is a mixed mode of brittle fracture and dimple fracture.

Besides the effect of brittle metallic compound, the induced residual stresses play an important role in the joining of dissimilar materials, which strongly affects the strength of joints. During the cooling process, the contraction of 316L steel is larger than that of the W owing to different CTE, which causes residual stresses located adjacent to W (the low CTE material). In addition, the brittle nature of tungsten also may result in fracture at the W substrate.

4. Conclusion

The effect of copper interlayer on the microstructure and mechanical property of 316L/W brazed joints are investigated. The following conclusions are summarized.

1. The bonding between tungsten and 316L steel can be successfully achieved by brazing without microcracks and unbounded regions at the interfaces. No intermetallic compound is formed at 316L/BNi-2 interface and BNi-2/Cu interface due to the good compatibility between Fe and Ni, Ni and Cu; NiW analyzed by XRD is observed at W/BNi-2 interface.

2. The substantial changes of microhardness are attributed to the formation of solid solution and intermetallic compound. The maximum microhardness is located at the interface next to W for W/Cu/316L joint and W/316L joint, respectively.

3. The average shear strength of the brazed joints increased due to adding the Cu foil interlayer, and the shear strength value is also affected by the thickness of Cu foil interlayer; the appropriate thickness of Cu foil interlayer is approximately 0.1 mm to reach the maximum joint shear strength. All shear testing specimens fractured in W near to the W/BNi-2 interface. The fracture mode of 316L/W is brittle fracture, while the fracture mode of 316L/Cu/W is a mixed mode of brittle fracture and dimple fracture.

Acknowledgment

References

1. Z.H. Zhong, H. Jung, T. Hinoki, and A. Kohyama, Effect of Joining Temperature on the Microstructure and Strength of Tungsten/Ferritic Steel Joints Diffusion Bonded with a Nickel Interlayer, *J. Mater Process. Tech*, 2010, **210**, p 1805–1810

2. W.W. Basuki, R. Dahm, and J. Aktaa, Thermomechanical Analysis of Diffusion-Bonded Tungsten/EUROFER97 with a Vanadium Interlayer, *J. Nucl. Mater.*, 2014, **455**, p 635–639

3. D. Stork, P. Agostini, J.L. Boutard, and D. Buclcthorpe, Developing Structural, High-Heat Flux and Plasma Facing Materials for a Near-Term DEMO Fusion Power Plant: The EU Assessment, *J. Nucl. Mater.*, 2014, **455**, p 277–291

4. P. Norajitra, R. Giniyatulin, and W. Krauss, He-Cooled Divertor Development Towards DEMO, *Fusion Sci. Technol.*, 2009, **56**, p 1013–1017

5. R.L. Klueh and A.T. Nelson, Ferritic/Martensitic Steel for Next-Generation Reactors, *J. Nucl. Mater.*, 2007, **371**, p 37–52

6. Z.H. Zhong, H. Tatsuya, and N. Takashi, Microstructure and Mechanical Properties of Diffusion Bonded Joints Between Tungsten and F82H Steel Using a Titanium Interlayer, *J. Alloy. Compd.*, 2010, **489**, p 545–551

7. W.W. Basuki and J. Aktaa, Investigation of Tungsten/Eurofer97 Diffusion Bonding Using Nb Interlayer, *Fusion Eng. Des.*, 2011, **86**, p 2585–2588

8. Y.Z. Ma, Y.Y. Wang, W.S. Liu, and Q.S. Cai, Interface Microstructure and Mechanical Properties of Diffusion Bonded Joints Between Tungsten and Ferritic steel with Vanadium Interlayer, *Trans. Weld. Insitu. China*, 2013, **34**, p 17–20

9. W.W. Basuki and J. Ktaa, Investigation on the Diffusion Bonding of Tungsten and EUROFER97, *J. Nucl. Mater.*, 2011, **417**, p 524–527

10. Z.H. Zhong, T. Hinoki, and A. Kohyama, Effect of Holding Time on the Microstructure and Strength of Tungsten/Ferritic Steel Joints Diffusion Bonded with a Nickel Interlayer, *Mater. Sci. Eng., A*, 2009, **518**, p 167–173

11. B.A. Kalin, V.T. Fedotov, O.N. Sevrjukov, A. Moeslang, and M. Rohde, Development of Rapidly Quenched Brazing Foils to Join Tungsten Alloys with Ferritic Steel, *J. Nucl. Mater.*, 2004, **329-333**, p 1544–1548

12. B.A. Kalin, V.T. Fedotov, O.N. Sevrjukov, A.N. Kalashnikov, A.N. Suchkov, A. Moeslang, and M. Rohde, Development of Brazing Foils to Join Monocrystalline Tungsten Alloys with ODS-EUROFER Steel, *J. Nucl. Mater.*, 2007, **367-370**, p 1218–1222

13. T. Chehtov, J. Aktaa, and O. Kraft, Mechanical Characterization and Modeling of Brazed EUROFER-Tungsten-Joints, *J. Nucl. Mater.*, 2007, **367-370**, p 1228–1232

14. S. Saito, K. Fukaya, S. Ishiyama, and K. Sato, Mechanical Properties of HIP Bonded W and Cu-Alloys Joint for Plasma Facing Components, *Nucl. MaXer*, 2002, **307-311**, p 1542–1546

15. W.S. Liu, S.H. Liu, and Y.Z. Ma, Microstructure and Properties of Tungsten/Steel Joint Brazed with Ni-Based Foil-Type Filler, *Trans. Nonferr. Met. Soc. China*, 2014, **24**(12), p 3051–3058

16. L. Sun and Y. Qin, Effect of alloy Element Cu on Microstructure and Mechanical Properties of Stainless Steel Brazed Joints, *Hot Work Technol*, 2014, **43**(23), p 68–71

17. H. Baker, *ASM Handbook, Volume 3: Alloy Phase Diagrams [M]*, ASM International Press, USA, 1992

18. M. Kajihara, Analysis of Kinetics of Reactive Diffusion in a Hypothetical Binary System, *Acta Mater.*, 2004, **52**, p 1193–1200

19. M. Kajihara, Relationship Between Temperature Dependence of Interdiffusion and Kinetics of Reactive Diffusion in a Hypothetical Binary System, *Mater. Sci. Eng., A*, 2005, **403**, p 234–240

20. K.E. Poulsen, S. Rubaek, and E.W. Langer, A New Intermetallic Phase in the W-Ni System, *Scr. Met.*, 1974, **8**, p 1297–1300

21. S. Inomataa and M. Kajihara, Solid-State Reactive Diffusion Between Ni and W, *J Alloy Compd*, 2011, **509**, p 4958–4966

22. S. Dconzone, D.P. Butt, and A.H. Bartlett, Joining $MoSi_2$ to 316L Stainless Steel, *J. Mater. Sci.*, 1997, **32**(13), p 3369–3374

23. J.X. Zhang, R.S. Chandel, Y.Z. Chen, and H.P. Seow, Effect of Residual Stress on the Strength of an Alumina-Steel Joint by Partial Transient Liquid Phase (PTLP) Brazing, *J. Mater. Process. Technol.*, 2002, **122**(2), p 220–225

24. J.W. Park, P.F. Mendez, and T.W. Eagar, Strain Energy Distribution in Ceramic-to-Metal Joints, *Acta Mater.*, 2002, **50**, p 883–899

25. J.W. Park and T.W. Eagar, Strain Energy Release in Ceramic-to-Metal Joints with Patterned Interlayers, *Scr. Mater.*, 2004, **50**, p 555–559

26. Y. Zhu, D. Qi, and W. Guo, The Braze Joint Between Al_2O_3 to 1Cr18Ni9Ti Using a Nickel Foam, *Weld. World*, 2015, **59**(4), p 491–496

27. K.M. Erskine, A.M. Meier, V.V. Joshi, and S.M. Pilgrim, The Effect of Braze Interlayer Thickness on the Mechanical Strength of Alumina Brazed with Ag-CuO Braze Alloys, *Adv. Eng. Mater.*, 2014, **16**(12), p 1442–1447